



## OPEN ACCESS

## EDITED BY

Ratnakar Potla,  
Genentech Inc., United States

## REVIEWED BY

Ilya D. Klabukov,  
National Medical Research Radiological Center,  
Russia  
Irene Cantarero,  
University of Cordoba, Spain

## \*CORRESPONDENCE

Scott T. Wood,  
✉ swood25@une.edu

RECEIVED 18 February 2025

ACCEPTED 27 March 2025

PUBLISHED 09 April 2025

## CITATION

Mirazi H and Wood ST (2025) Microfluidic chip-based co-culture system for modeling human joint inflammation in osteoarthritis research. *Front. Pharmacol.* 16:1579228. doi: 10.3389/fphar.2025.1579228

## COPYRIGHT

© 2025 Mirazi and Wood. This is an open-access article distributed under the terms of the [Creative Commons Attribution License \(CC BY\)](https://creativecommons.org/licenses/by/4.0/). The use, distribution or reproduction in other forums is permitted, provided the original author(s) and the copyright owner(s) are credited and that the original publication in this journal is cited, in accordance with accepted academic practice. No use, distribution or reproduction is permitted which does not comply with these terms.

# Microfluidic chip-based co-culture system for modeling human joint inflammation in osteoarthritis research

Hosein Mirazi<sup>1</sup> and Scott T. Wood<sup>1,2,3\*</sup>

<sup>1</sup>Department of Nanoscience and Biomedical Engineering, South Dakota School of Mines and Technology, Rapid City, SD, United States, <sup>2</sup>Portland Laboratory for Biotechnology and Health Sciences, University of New England, Portland, ME, United States, <sup>3</sup>Department of Biomedical Sciences, University of New England, Biddeford, ME, United States

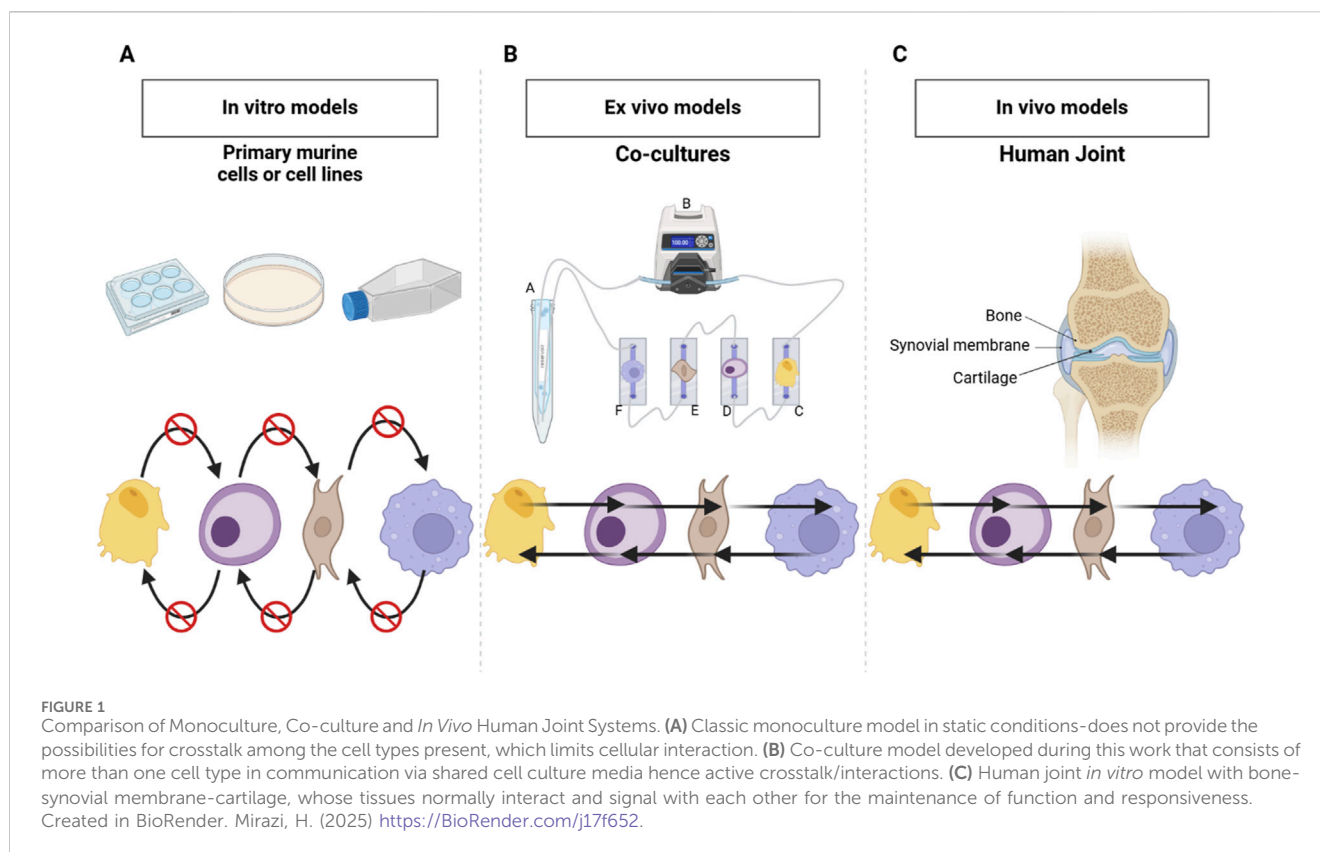
Here we present a microfluidic model that allows for co-culture of human osteoblasts, chondrocytes, fibroblasts, and macrophages of both quiescent (M0) and pro-inflammatory (M1) phenotypes, maintaining initial viability of each cell type at 24 h of co-culture. We established healthy (M0-based) and diseased (M1-based) joint models within this system. An established disease model based on supplementation of IFN- $\gamma$  and lipopolysaccharide in cell culture media was used to induce an M1 phenotype in macrophages to recapitulate inflammatory conditions found in Osteoarthritis. Cell viability was assessed using NucBlue™ Live and NucGreen™ Dead fluorescent stains, with mean viability of  $83.9\% \pm 14\%$  and  $83.3\% \pm 12\%$  for healthy and diseased models, respectively, compared with  $93.3\% \pm 4\%$  for cell in standard monoculture conditions. Cytotoxicity was assessed via a lactate dehydrogenase (LDH) assay and showed no measurable increase in lactate dehydrogenase release into the culture medium under co-culture conditions, indicating that neither model promotes a loss of cell membrane integrity due to cytotoxic effects. Cellular metabolic activity was assessed using a PrestoBlue™ assay and indicated increased cellular metabolic activity in co-culture, with levels  $5.9 \pm 3.2$  times mean monolayer cell metabolic activity levels in the healthy joint model and  $5.3 \pm 3.4$  times mean monolayer levels in the diseased model. Overall, these findings indicate that the multi-tissue nature of *in vivo* human joint conditions can be recapitulated by our microfluidic co-culture system at 24 h and thus this model serves as a promising tool for studying the pathophysiology of rheumatic diseases and testing potential therapeutics.

## KEYWORDS

osteoarthritis, microfluidic co-culture, human joint model, *in vitro* disease modeling osteoblasts, chondrocytes, macrophages, fibroblasts osteoarthritis, microfluidic co-culture system

## Introduction

Osteoarthritis (OA) is a crippling health condition generally characterized by chronic joint pain, degeneration of articular cartilage, synovitis, and bone remodeling (Tong et al., 2022). OA affects over 520 million people worldwide, and frequently progresses to the point of requiring joint replacement in late stages of the disease because no disease-modifying OA drugs have yet received regulatory approval (Grässel and Muschter, 2020; Long et al., 2022).



An important limitation of most prior studies is that, as illustrated in Figure 1, the monoculture models used in those studies are devoid of cellular crosstalk, which is an important constituent of the joint as an organ (Loeser et al., 2012). The development of preclinical *in vitro* models reproducing the complexity of human joint diseases constitute an important trend in OA research, yet current models are still limited in their capacity to recapitulate the complex multicellular nature of human joints, hindering the development of an efficient therapy for OA (Cope et al., 2019; Domínguez-Oliva et al., 2023; Malfait and Little, 2015; Perisin and Sund, 2018; Swearingen, 2018; Xie et al., 2018).

*In vivo* models, though providing valuable insights into OA, often fail to accurately mimic human physiology due to limitations in replicating the complex interactions between joint tissues (Cope et al., 2019). This often leads to inconsistent and non-predictive outcomes in drug development studies (Dou et al., 2023; Guo et al., 2022; Zaki et al., 2022). Existing *in vitro* models, while more advanced, are generally restricted to the cartilage compartment, and co-culturing of key cell types involved in OA—such as osteoblasts, chondrocytes, fibroblasts, and macrophages—is uncommon (Banh et al., 2022; Haltmayer et al., 2019; He et al., 2020; Piroso et al., 2021; Salgado et al., 2021). One major challenge contributing to this gap is that these different cell types have distinct media requirements, making it difficult to maintain all cells under the same conditions (Weiskirchen et al., 2023). Additionally, some multi-cell models rely on induced pluripotent stem cells (iPSCs) instead of using patient-derived cell types representative of mature cells from each specific tissue, which limits the accuracy of disease representation (Li et al., 2023; Makarczyk et al., 2023).

Unlike classical mono-culture models, co-culture systems allow interactions to occur between cell types, a situation much more similar to the *in vivo* environment of human joints. The use of advanced bioengineered models, such as microphysiological systems (MPSs), which includes organoids and organs on chips, likely represents the future of OA research (Banh et al., 2022; Goers et al., 2014; Hofer and Lutolf, 2021). These systems are designed to capture these intercellular interactions and provide a more physiologically relevant translation of human physiology than earlier approaches (McNerney et al., 2021; Palasantzas et al., 2023; Rothbauer et al., 2021). Figure 2 illustrates different approaches to disease modeling, including the use of immune cells, such as macrophages, to simulate inflammatory conditions. A model with the involvement of all the key cell types of a human joint—osteoblasts, chondrocytes, fibroblasts, and macrophages—could mark a pivotal advance leading to fundamental changes in our understanding of the pathogenesis of OA and other complex joint diseases.

The most critical limitation of most of the multi-cell models available, especially the ones based on iPSCs, is that they generally either do not differentiate precisely into the highly specialized cell types that are critical for studying the osteoarthritic joint environment, most notably adult articular chondrocytes. As most iPSC-based models are cytokine-driven, their differentiation is susceptible to be driven to inhomogeneous and non-physiological phenotypes, and hence it can be difficult to accurately recapitulate key characteristics of cells participating in OA pathogenesis (Kao et al., 2023; Zhou et al., 2021). Some co-culture models have been published that include a limited number of human joint cell types,

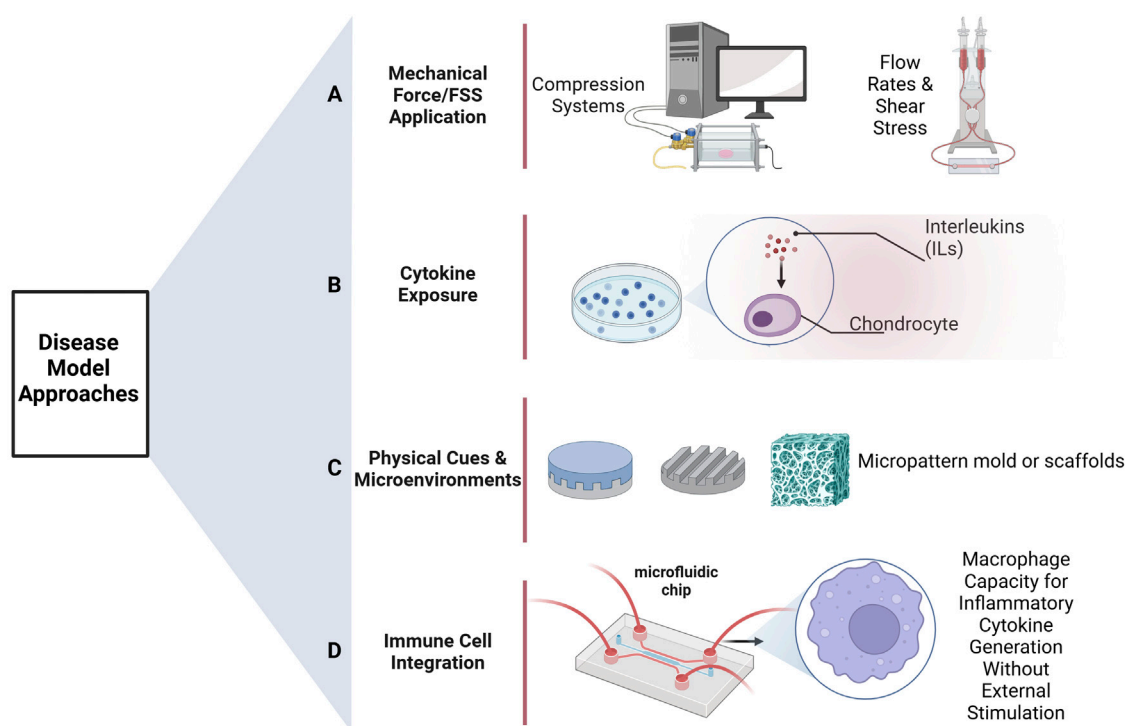


FIGURE 2

Methods of disease model development. (A) Group of methods relies on flow rates or applies mechanical forces/fluid shear stresses as a method of stimulation to the cells. (B) Inflammatory cytokines, such as interleukins or other stimulators, are used directly on the cells for inducing disease states. (C) Physical stimuli or microenvironments—for example, various scaffolds—are used with the express intention of directing and eliciting from the cells responses that are characteristic of diseases. (D) To simulate conditions seen in inflammatory diseases, the system is treated with immune cells, including macrophages, which stimulate the secretion of inflammatory cytokines. Created in BioRender. Mirazi, H. (2025) <https://BioRender.com>.

but to date, no studies have been published establishing co-culture conditions to mimic the joint microenvironment using cells from three different joint tissues, the most universal of which are bone, cartilage, and synovium (Awad et al., 2023; Kao et al., 2023). This has created a need for an integrated system bringing together cells from these essential components of the joint for capturing the multifactorial nature of OA, and of the joint as an organ, more effectively.

To address the challenges associated with co-culturing bone, cartilage, and synovium cells together, we utilized a microfluidic co-culture system designed to replicate the complex paracrine dynamics of the human joint environment. Unlike traditional static models, our system enables these distinct cell types to interact under controlled flow conditions using a combined cell culture media, allowing us to overcome the limitations of differing media requirements. The goal of this study was to create a biologically relevant platform that integrates osteoblasts, chondrocytes, fibroblasts, and both quiescent (M0) and pro-inflammatory (M1) macrophages as illustrated in Figure 3, thereby mimicking paracrine cellular interactions under both healthy and diseased conditions. We hypothesized that, on average, cell viability and metabolic activity could be maintained at  $\geq 70\%$ – $80\%$  of baseline monoculture levels through this shared microenvironment that promotes paracrine crosstalk between cell types. By successfully replicating these paracrine

interactions using human patient-derived cells, we provide the foundation for a novel system capable of advancing the understanding of OA pathogenesis and enabling the testing of therapeutic interventions in a reliable and replicable manner.

## Materials and methods

### Cell culture

Primary human osteoblasts (HOBs) isolated from the cancellous bone of the femoral head of an 85-year-old Caucasian female were obtained from PromoCell (Heidelberg, Germany) and cultured per manufacturer recommendations. Briefly, HOBs were expanded in Osteoblast Growth Medium in T-75 flasks at  $37^{\circ}\text{C}$  in a  $5\% \text{CO}_2$  humidified incubator and used between passages four to six. Following expansion, HOBs were seeded in microchannels at a density of  $40,000 \text{ cells/cm}^2$  for experimentation.

Primary human chondrocytes (HCHs) isolated from the cartilage of the tibial head of a 74-year-old female were obtained from PromoCell and cultured per manufacturer recommendations. HCHs were expanded in Chondrocyte Growth Medium in T-75 flasks at  $37^{\circ}\text{C}$  in a  $5\% \text{CO}_2$  humidified incubator and used between passages three to five. Following expansion, HCHs were seeded in microchannels at a density of  $80,000 \text{ cells/cm}^2$  for experimentation.

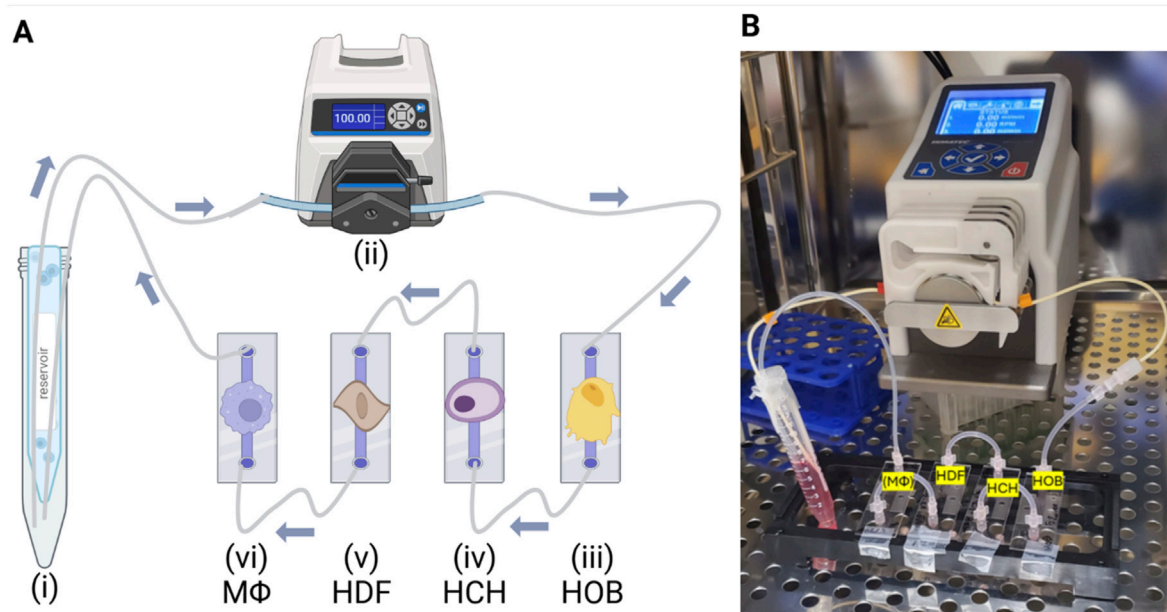


**FIGURE 3**  
Experimental Setup and Workflow. (A) Illustration and (B) Photo of experimental setup placed inside the incubator, where the microfluidic system operated under controlled conditions for the duration of the experiment. Created in BioRender. Mirazi, H. (2025) <https://BioRender.com/u04h894>.

Primary human dermal fibroblasts (HDFs) isolated from adult skin (female, 49 years old) were obtained from the American Type Culture Collection (ATCC) and cultured per manufacturer recommendations. Briefly, HDFs were expanded in Dulbecco's Modified Eagle's Medium (DMEM) supplemented with 10% fetal bovine serum (FBS) and 1% penicillin-streptomycin (P/S) in T-75 flasks, incubated at 37°C in a 5% CO<sub>2</sub> humidified environment and used between passages four to six. Following expansion, HDFs were seeded in microchannels at a density of 40,000 cells/cm<sup>2</sup> for subsequent experimentation.

THP-1 monocytes isolated from the peripheral blood of a one-year-old male patient with acute monocytic leukemia were obtained from ATCC and cultured per manufacturer recommendations. THP-1s were expanded in RPMI-1640 Medium supplemented with 10% fetal bovine serum (FBS), 1% penicillin-streptomycin (P/S), 2 mM L-glutamine, 10 mM (2-[4-(2-hydroxyethyl) piperazin-1-yl] ethanesulfonic acid) (HEPES), 1 mM sodium pyruvate, 4.5 g/L glucose, and 1.5 g/L sodium bicarbonate. THP-1 cells were maintained in T-25 flasks at a seeding density of 4.0 × 10<sup>5</sup> viable cells/mL, reaching approximately 1.4 × 10<sup>6</sup> viable cells/mL after 6 days with media addition, under incubation at 37°C in a 5% CO<sub>2</sub> humidified environment.

Prior to experimentation, THP-1 cells were differentiated into either the M0 (i.e., quiescent) or M1 (i.e., pro-inflammatory) macrophage (MΦ) phenotype, following the protocol previously described (Baxter et al., 2020). Briefly, monocytes were seeded in microchannels at 75,000 cells/cm<sup>2</sup>, incubated with 50 nM Phorbol 12-Myristate 13-Acetate (PMA) for 48 h, and then allowed to rest in PMA-free medium for an additional 24 h to differentiate into THP-1-derived M0-type macrophages (M0MΦs). To induce the pro-inflammatory M1 phenotype, M0MΦs were treated for 24 h with 20 ng/mL human

interferon gamma (IFNγ) and 100 ng/mL lipopolysaccharide (LPS) derived from *Escherichia coli* O111.

## Microfluidic co-culture

A μ-Slide I Luer ibiTreat (Ibidi, Germany) system was utilized for cultivating osteoblasts, chondrocytes, fibroblasts, and macrophages under controlled flow conditions, regulated by a Masterflex® Ismatec® Reglo ICC Peristaltic Pump. Cells were seeded and allowed to attach overnight in a 5% CO<sub>2</sub> incubator at 37°C. Once attachment was confirmed, the μ-Slide I Luer units were connected into a fluidic circuit, and shared media was circulated through the system for 2 h, at a shear stress of 0.05 dyn/cm<sup>2</sup> as illustrated in Figure 3. This process allowed thorough mixing, facilitating nutrient exchange and communication among the cells. After 2 h of mixing under flow, circulation was stopped, and the cells were allowed to remain in the shared media for an additional 24 h without active flow. This period aimed to enable paracrine interactions while also while enabling media sampling specific to each cell type. Following the 24-h static flow co-culture period, cell viability, cytotoxicity, and metabolic activity were assessed. These assays were selected to provide comprehensive insights into cell.

## Viability assessment

Cell viability was assessed using the ReadyProbes™ Cell Viability Blue/Green Imaging Kit (Invitrogen). NucBlue™ Live stained all cell nuclei (displayed as green), while NucGreen™ Dead selectively labeled dead cells (displayed as magenta). Upon



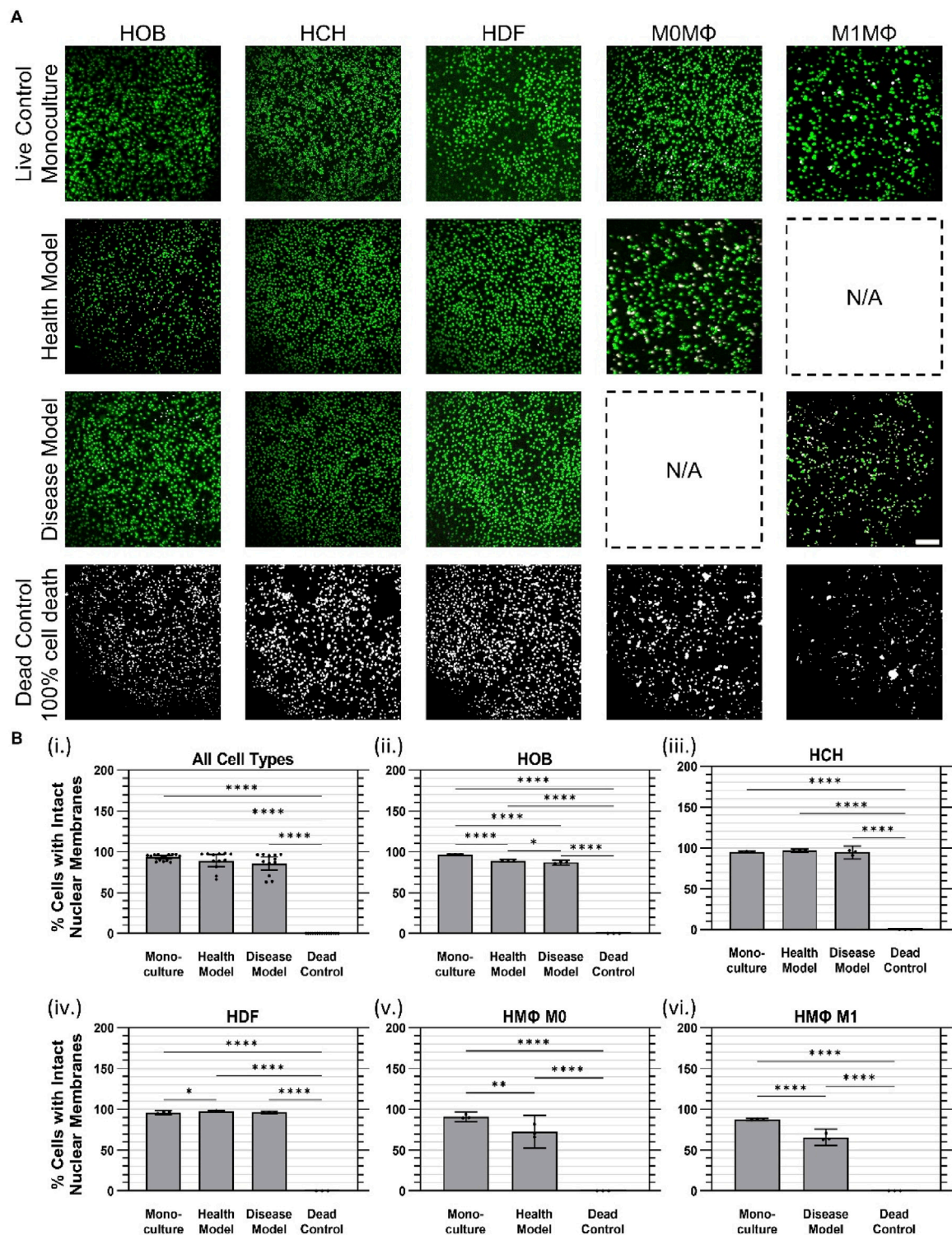


**FIGURE 4**  
Cell viability was largely maintained at 24 h of co-culture in health and disease models. **(A)** Representative images of live (green) and dead (white) cell nuclei. **(B)** Quantified cell viability data for (i) Aggregated data across all cell types in monoculture, health co-culture, disease co-culture models, and dead controls; (ii) osteoblasts (HOB); (iii) chondrocytes (HCH); (iv) fibroblasts (HDF); (v) quiescent (M0) macrophages, i.e., Health Model; and (vi) pro-inflammatory (M1) macrophages, i.e., Disease Model. Data are mean  $\pm$  95% CI. \*  $p < 0.05$ , \*\*  $p < 0.01$ , \*\*\*  $p < 0.0001$ . Scale bar: 200  $\mu$ m.

overlay, live cells appeared with green nuclei, dead cells exhibited white nuclei, and magenta-stained nuclei indicated compromised or damaged cells (Figure 4A). Samples were incubated with two drops

of each reagent per mL of culture media for 20 min at 37°C. Fluorescence microscopy was performed using an Olympus IX71 microscope equipped with a UPLFLN  $\times 10$  objective and an

Andor iXon Ultra EMCCD camera (Andor) to capture high-resolution images for quantitative analysis. For this study, the monoculture condition served explicitly as a live-cell positive control, representing standard healthy cell viability. For a negative (dead) control, cells under monoculture conditions were lysed according to the manufacturer's protocol using 10X lysis buffer for 45 min, resulting in 100% cell death.

## Metabolic activity assessment

Metabolic activity, a reliable indicator of cell viability, was assessed using PrestoBlue™ HS Cell Viability Reagent (Invitrogen) (Boncler et al., 2014; Xu et al., 2015). This reagent, which relies on the reduction of resazurin to resorufin by metabolically active cells, provided a measure of cellular health (Martín-Navarro et al., 2014).

PrestoBlue™ reagent was diluted into the combined cell culture media according to the manufacturer's instructions and introduced into the microfluidic chambers. Following incubation at 37°C for 2 h, fluorescence measurements were performed at excitation/emission wavelengths of 560/590 nm using a SpectraMax i3 plate reader (Molecular Devices, LLC., San Jose, CA). Monoculture conditions served as a positive control, representing the baseline metabolic activity of healthy individual cell populations. In contrast, the dead control group was generated by lysing cells under static monoculture conditions using  $\times 10$  lysis buffer, representing a condition of complete loss of metabolic activity.

## Cytotoxicity assessment

Cytotoxicity was evaluated using the CyQUANT™ LDH Cytotoxicity Assay (Invitrogen) to measure cell membrane integrity under co-culture conditions. LDH release into the culture medium indicates compromised membrane integrity associated with cell death or damage. For the dead control group (maximum LDH release), cells cultured under static monoculture conditions were lysed by adding 10  $\mu$ L of  $\times 10$  Lysis Buffer per well, followed by gentle mixing to ensure complete lysis, according to the manufacturer's instructions. Media samples from both the microfluidic co-culture system and static monoculture dead controls were then collected and analyzed using a SpectraMax i3 plate reader at excitation/emission wavelengths of 560/590 nm. The monoculture condition served as a low-cytotoxicity baseline control, while the dead control group, generated by lysis with 10  $\mu$ L of  $\times 10$  Lysis Buffer under static conditions, represented maximum LDH release.

## Ethical considerations

Primary human cells utilized in this study (osteoblasts, chondrocytes, fibroblasts, and macrophages) were commercially sourced from established vendors (PromoCell and ATCC). These cells are anonymized and obtained with documented informed consent and ethical clearance provided by the suppliers.

Therefore, additional institutional ethical approval was not required for the current study.

## Statistical analysis

Data from three independent experiments were analyzed for all statistical analyses. Effects of culture conditions were determined using one-way ANOVA with Tukey multiple comparisons *post hoc* test with a single pooled variance. Effects were confirmed using a significance level of  $\alpha = 0.05$ . Data are represented as mean  $\pm$  95% confidence interval (95% CI). All statistical analyses were performed using GraphPad Prism 10.3.1.

## Results

### Viability

Cell viability was assessed using a ReadyProbes™ Cell Viability Imaging Kit to distinguish cells with intact nuclear membranes (i.e., live cells) from cells with disrupted nuclear membranes (i.e., dead cells), as described above. Dead controls were generated by treating cells that had been plated under monoculture conditions with 10X lysis buffer for 45 min to achieve complete cell death. Overall, when considering all cell types together within each culture condition, no measurable (i.e., statistically significant) differences in cell viability were observed between the monoculture (mean  $93.3\% \pm 3.8\%$  SD) and co-culture conditions ( $89.2\% \pm 11\%$  health model,  $85.9\% \pm 13\%$  disease model), as indicated in Figure 4Bi. However, measurable differences ( $p < 0.0001$ ) were found between the dead control group (no detectable nuclei remained under any condition) and the monoculture and co-culture models.

For HOBs, cell viability in monoculture ( $97.0\% \pm 0.1\%$ ) and in health ( $89.2\% \pm 0.6\%$ ) and disease ( $87.0\% \pm 1.2\%$ ) co-culture models were all substantially higher than the dead control group (0%). A marginal but measurable difference in cell viability between health and disease models was observed (Figure 4Bii). For HCHs, no measurable difference in cell viability was found between monoculture ( $95.1\% \pm 0.5\%$ ) and health ( $97.2\% \pm 0.8\%$ ) or disease ( $94.4\% \pm 3.2\%$ ) co-culture models. However, all conditions showed substantially higher viability than the dead control group (0%); Figure 4Biii). HDF cell viability was marginally but measurably higher in the health co-culture model ( $97.6\% \pm 0.6\%$ ) compared to monoculture ( $96.0\% \pm 0.9\%$ ), while no measurable difference was observed between health and disease co-culture models ( $96.3\% \pm 0.6\%$ ). All conditions had higher viability compared to the dead control group (0%) (Figure 4Biv); For M0 quiescent macrophages, viability was measurably higher in monoculture ( $90.9\% \pm 2.4\%$ ) compared to the health co-culture model ( $72.8\% \pm 8.0\%$ ) and both conditions had substantially higher viability than the dead control group (0%) (Figure 4Bv); For M1 pro-inflammatory macrophages, viability in monoculture ( $87.6\% \pm 0.6\%$ ) and disease co-culture model ( $65.8\% \pm 4.1\%$ ) were both lower than for other cell types, but were still substantially higher than the dead control group (0%), with a measurable difference between monoculture and disease co-culture models (Figure 4Bvi).

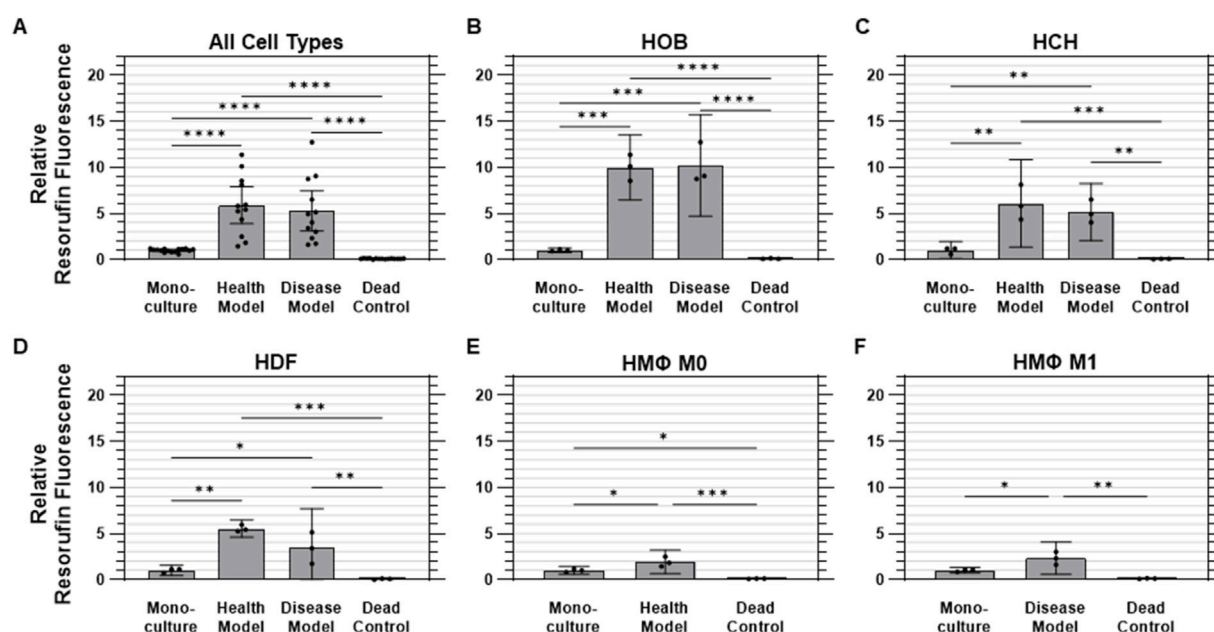


**FIGURE 5** Metabolic activity was elevated under co-culture conditions. Quantified metabolic activity data (relative fluorescence) for (A) aggregated data across all cell types in monoculture, health co-culture, disease co-culture models, and dead controls; (B) osteoblasts (HOB); (C) chondrocytes (HCH); (D) fibroblasts (HDF); (E) quiescent (M0, i.e., Health Model) macrophages; and (F) pro-inflammatory (M1, i.e., Disease Model) macrophages. Data are mean  $\pm$  95% CI relative to monoculture. \* $p$  < 0.05, \*\* $p$  < 0.01, \*\*\* $p$  < 0.001, \*\*\*\* $p$  < 0.0001.

## Metabolic activity

Cell metabolic activity was assessed using the PrestoBlue™ assay, with levels of resorufin fluorescence relative to monoculture conditions (mean  $1.00 \pm 0.19$  RFU [SD]) serving as an indicator of cell viability. Overall, the health co-culture model exhibited the highest metabolic activity, with a mean relative fluorescence of  $5.89 \pm 3.17$  RFU, followed by the disease co-culture model at  $5.28 \pm 3.42$  RFU. In contrast, the dead control group showed minimal metabolic activity, with a maximum fluorescence of  $0.10 \pm 0.03$  RFU (Figure 5A).

For HOBs, both co-culture models were found to have measurably higher metabolic activity than monoculture and dead control conditions. The health co-culture model showed a mean fluorescence of  $10.0 \pm 1.4$  times those of monoculture HOBs ( $1.00 \pm 0.09$  RFU), while the disease co-culture model demonstrated a roughly equivalent value of  $10.2 \pm 2.2$  times monoculture values. Dead controls showed minimal metabolic activity at  $0.11 \pm 0.03$  RFU (Figure 5B). For HCHs, both co-culture models were also found to have measurably higher metabolic activity than monoculture ( $1.00 \pm 0.4$  RFU) and dead control ( $0.08 \pm 0.03$  RFU) conditions. The health co-culture model displayed the highest metabolic activity of all conditions, with a mean fluorescence of  $6.09 \pm 1.9$  RFU, followed by the disease co-culture model at  $5.16 \pm 1.2$  RFU, although the difference between these values was not found to be statistically measurable (Figure 5C). Both co-culture models were found to have measurably higher metabolic activity than monoculture ( $1.00 \pm 0.2$  RFU) and dead control ( $0.07 \pm 0.04$  RFU) conditions for HDFs as well. As was found for HOBs, the health co-culture model exhibited the highest metabolic activity for HDFs, with a mean

fluorescence of  $5.54 \pm 0.4$  RFU, followed by the disease co-culture model at  $3.44 \pm 1.7$  RFU, with the difference between the two not found to be statistically measurable (Figure 5D). For M0 macrophages, the health co-culture model exhibited a mean metabolic activity of  $1.92 \pm 0.5$  times that of monoculture ( $1.00 \pm 0.2$  RFU). The M0 dead controls exhibited minimal activity at  $0.10 \pm 0.02$  RFU. All M0 conditions were found to be measurably different from one another (Figure 5E). M1 macrophages in the disease co-culture model displayed a mean metabolic activity ( $2.33 \pm 0.7$  RFU) measurably higher than those of M1 macrophages in either monoculture ( $1.00 \pm 0.1$  RFU) or dead control ( $0.13 \pm 0.03$  RFU) conditions (Figure 5F).

## Cytotoxicity

Cytotoxicity was evaluated using the lactate dehydrogenase (LDH) assay, which measures the release of intracellular LDH from cells as an indicator of compromised membrane integrity due to cell damage or death. No measurable differences were observed between monoculture and either co-culture model for any cell type, while all three culture conditions were found to release measurably less LDH into conditioned media than the cells in the dead controls for all cell types except HDFs, which were found to have an abnormally high degree of variability in the dead control samples. On the whole, cells cultured under monoculture conditions released  $86.2\% \pm 8.3\%$  less (i.e.,  $0.138 \pm 0.083$  times as much) LDH than dead control cells ( $1.00 \pm 0.17$ ) on average, while those in the health and disease co-culture models released  $83.7\% \pm 10.9\%$  and  $87.4\% \pm 9.6\%$  less LDH than dead control cells, respectively (Figure 6A).



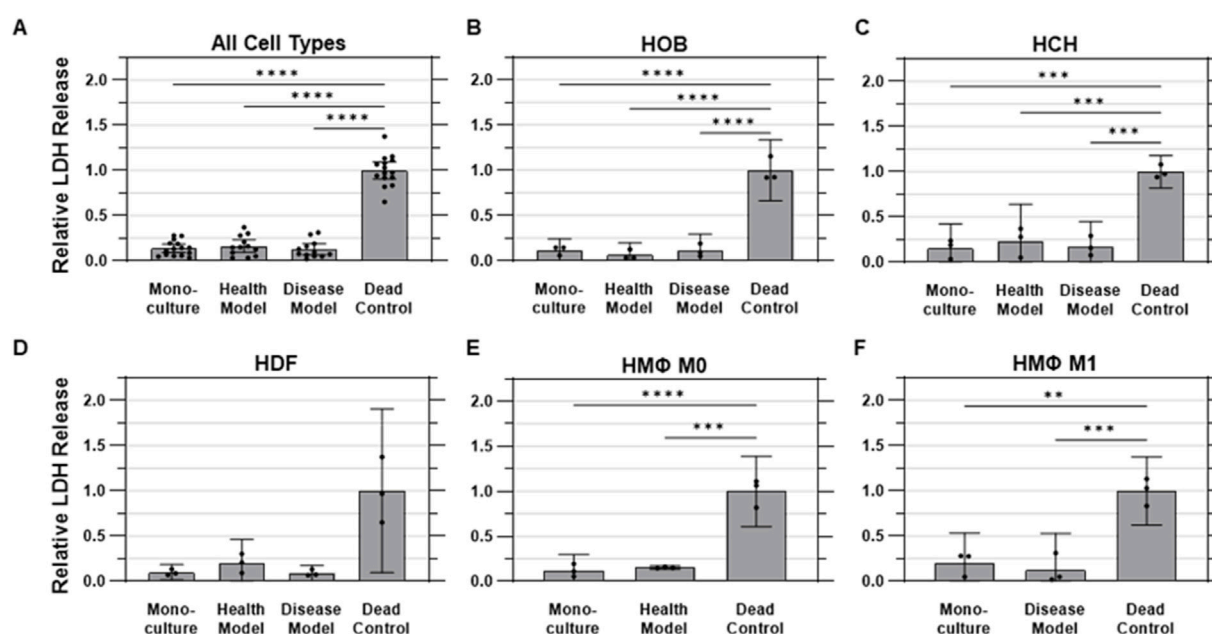


FIGURE 6

Membrane integrity was not substantially impacted by co-culture. Quantified LDH release into conditioned media, representing cell membrane integrity across various experimental conditions. (A) Aggregated data across all cell types in monoculture, health co-culture, disease co-culture models, and dead controls; (B) osteoblasts (HOB); (C) chondrocytes (HCH); (D) fibroblasts (HDF); (E) quiescent (M0, i.e., Health Model) macrophages; and (F) pro-inflammatory (M1, i.e., Disease Model) macrophages. Data are mean  $\pm$  95% CI relative to dead controls.

For HOBs, the dead control cells exhibited the highest LDH release levels, as expected, with a standard deviation of 10% of the mean value. The monoculture condition showed a substantially lower amount of LDH release, at  $12\% \pm 5\%$  as much as the dead control, while the health co-culture model had an even lower, but not statistically different, value of  $6.5\% \pm 5.4\%$  as much as the dead control. The disease model exhibited an LDH release of  $11.2\% \pm 7.3\%$  of dead control levels (Figure 6B). For HCHs, the dead control again had the highest normalized LDH release, with a standard deviation of 7% of the mean value. The health co-culture model exhibited LDH release of  $23.4\% \pm 0.16\%$  as much as dead control cells, followed by the disease co-culture model at  $17.5\% \pm 11\%$  and monoculture at  $15.3\% \pm 11\%$  of dead control values (Figure 6C). The dead control also displayed the highest amount of LDH release for HDFs, with a standard deviation of 36% of the mean value. The monoculture, health model, and disease model conditions exhibited LDH release levels of  $9.8\% \pm 3\%$ ,  $19.9\% \pm 11\%$ , and  $9.0\% \pm 3\%$  as much as the dead control, respectively (Figure 6D). For quiescent (M0) macrophages, the dead control cells released the highest amount of LDH, with a standard deviation of 16% of the mean value. The monoculture and health co-culture models showed lower LDH release levels of  $12.0\% \pm 7\%$  and  $15.4\% \pm 1\%$  of the levels of the dead control, respectively (Figure 6E). For pro-inflammatory (M1) macrophages, the dead control once again exhibited the highest LDH release, with a standard deviation of 15% of the mean value. The monoculture and disease model conditions were observed to release  $20.1\% \pm 13\%$  and  $12.7\% \pm 16\%$  as much LDH as the dead control, respectively (Figure 6F).

## Discussion

Traditional *in vitro* models lack the complexity required to accurately recapitulate the multi-tissue nature of joint tissue interactions, thus limiting their relevance for OA research. While co-culture systems involving two joint cell or tissue types (e.g., bone/cartilage) have been explored, they may still fail to capture the broader intercellular crosstalk seen *in vivo*. Here, we address this limitation by introducing a co-culture model with osteoblasts, chondrocytes, fibroblasts, and quiescent (M0) or pro-inflammatory (M1) macrophages, thereby providing a more representative platform for studying the pathophysiology of OA.

The primary goal of this study was to develop a microfluidic co-culture model that integrates osteoblasts, chondrocytes, fibroblasts, and macrophages, mimicking the complex environment of the human joint. Our aim was to demonstrate that, by sharing paracrine signals ostensibly representative of the *in vivo* condition, cells can maintain a healthy condition similar to monoculture even when all cell types share one combined culture medium rather *in lieu* of their typical individualized medium. By providing a controlled co-culture environment, this study aims to establish a new foundation for studying osteoarthritis pathophysiology and evaluating potential therapeutic interventions.

We hypothesized that this system would maintain cell viability, support metabolic activity, and preserve membrane integrity for all cell types under both healthy and disease-mimicking conditions. Specifically, we predicted that viability would remain above 80% across all cell types, metabolic activity in co-culture would be comparable to monoculture conditions, and cytotoxicity would



remain low and comparable to monoculture levels. Viability was successfully maintained across all conditions, with monoculture cells showing a mean viability of  $93.3\% \pm 3.8\%$ . The co-culture models exhibited slightly lower but comparable viability, with  $89.2\% \pm 11\%$  in the healthy model and  $85.9\% \pm 13\%$  in the disease model, all of which surpassed our hypothesized threshold of 80% viability (Figure 4B). Metabolic activity also met and exceeded expectations. Relative to monoculture ( $1.00 \pm 0.19$  RFU), metabolic activity was significantly elevated in the healthy co-culture model ( $5.89 \pm 3.17$  RFU) and disease co-culture model ( $5.28 \pm 3.42$  RFU), representing substantial increases in cellular metabolic function (Figure 5). Cytotoxicity, assessed through LDH release, showed no evidence of adverse effects due to co-culture conditions. Monoculture conditions released  $86.2\% \pm 8.3\%$  less LDH than dead control cells ( $1.00 \pm 0.17$  RFU), while the health and disease co-culture models released  $83.7\% \pm 10.9\%$  and  $87.4\% \pm 9.6\%$  less LDH, respectively (Figure 6).

While other models have co-cultured limited subsets of joint cells or tissues, such as osteoblasts with chondrocytes or cartilage with synovium, these models may fail to fully recapitulate the intercellular interactions present in the native joint microenvironment. To the best of our knowledge, no prior study has integrated four joint cell types into a single, shared microfluidic co-culture system. Furthermore, many of the previous studies relied on isolated tissue compartments or induced pluripotent stem cell (iPSC)-derived cells, which may not fully capture the physiological complexity of mature human cells. In contrast, our system incorporates primary human cells from bone, cartilage, synovium, and immune components, all of which interact within a shared medium under controlled flow conditions.

Although our current microfluidic co-culture model integrates four essential joint cell types osteoblasts, chondrocytes, fibroblasts, and macrophages (M0 and M1), it is important to recognize other immune cells, particularly mast cells (MCs) and M2 macrophages, that could significantly impact joint inflammation and OA pathology. Recent literature underscores the critical roles of these cells in modulating inflammation, cartilage metabolism, and overall joint homeostasis, thus emphasizing the potential benefits of incorporating these additional immune components in future iterations of our model.

Recent studies on tissue-engineered grafts suggest that the presence of chondrocytes can alter immune responses by promoting plasma cell infiltration and influencing mast cell activity. These cells contribute to inflammation through cytokine release and matrix degradation via MMPs. Additionally, mast cell-derived tryptase plays a key role in extracellular matrix remodeling and fibroblast activation. These findings further support the relevance of including mast cells and plasma cells in future co-culture models to better mimic the complex immune interactions in osteoarthritic joints (Klabukov et al., 2023).

Additional findings support the relevance of incorporating MC-driven interactions in advanced co-culture models to better reflect the complexity of OA pathophysiology, as studies highlight the critical role of mast cells (MCs) in modulating inflammation and interacting with key joint cell types, including T cells, fibroblasts, macrophages, osteoclasts, and osteoblasts. MC-derived mediators such as tryptase, TNF- $\alpha$ , and IL-6 contribute to synovial inflammation, fibroblast activation, chondrocyte damage, and bone remodeling (Hao et al., 2024).

While mast cells often contribute to inflammation, they also display immunomodulatory properties and support tissue homeostasis under certain conditions (Kilinc et al., 2022). MCs significantly influence joint inflammation and OA pathology through the release of various bioactive mediators, including histamine, serotonin, proteases (such as tryptase), lipid mediators (prostaglandins and leukotrienes), cytokines, chemokines, and reactive oxygen species. Improper activation of MCs is associated with several diseases, including allergic disorders (Galli et al., 2020). In OA specifically, MCs are typically classified into two subtypes based on their protease expression profiles: MCT cells, primarily expressing tryptase, and MCTC cells, co-expressing tryptase along with chymase and carboxypeptidase A3 (Cpa3) (Irani et al., 1986). Macrophages also significantly influence OA progression by secreting inflammatory cytokines, MMPs, growth factors, and TIMPs through autocrine and paracrine signaling (Zhang et al., 2020). They are primarily classified into pro-inflammatory M1 and anti-inflammatory M2 phenotypes. M1 macrophages release pro-inflammatory cytokines such as IL-6, TNF- $\alpha$ , IL-1, and IL-12 (Wang et al., 2014), exacerbating inflammation. In contrast, polarization to M2 macrophages helps alleviate osteoarthritis symptoms (Cao et al., 2023). Additionally, MCs further stimulate inflammation by secreting IL-1 $\beta$ , TNF- $\alpha$ , and IL-6, contributing to macrophage activation, osteoclast formation, and joint erosion (Cutolo et al., 2022).

Furthermore, chondrocytes are essential for maintaining joint integrity by producing an extracellular matrix primarily composed of aggrecan and type II collagen. However, their ability to regulate matrix synthesis and repair is disrupted during OA progression (Finnson et al., 2012; Martin and Buckwalter, 2002). Interestingly, MCs modulate chondrocyte metabolism by secreting TGF- $\beta$ , a key regulator of extracellular matrix synthesis and cartilage homeostasis (Zhen and Cao, 2014). Animal studies demonstrated that blocking TGF- $\beta$  signaling promotes cartilage degradation and accelerates OA progression (Shen et al., 2013); however, within the OA environment, elevated TGF- $\beta$  levels can paradoxically increase MMP-13 expression, causing further chondrocyte damage (Bailey and Alliston, 2022). Further research is needed to fully elucidate the complex role of MC-derived TGF- $\beta$  and TLR signaling in chondrocyte-mediated OA pathology.

Lin et al. developed a multi-chamber bioreactor to model the bone-cartilage interface using human bone marrow stem cell (hBMSC)-derived constructs. Separate medium streams created distinct chondral and osseous microenvironments, enabling targeted chondrogenic and osteogenic differentiation over a 4-week period (Lin et al., 2014). In a subsequent study, they utilized a dual-flow bioreactor to replicate the bone-cartilage interface using induced pluripotent stem cell-derived mesenchymal progenitor cells (iMPCs). The iMPCs were encapsulated within photo-crosslinked gelatin scaffolds and exposed to distinct chondro- and osteo-inductive cytokine conditions, with chondrogenic medium flowing from the top and osteogenic medium from the bottom (Lin et al., 2019). While both studies demonstrate progress in joint micro-physiological system development, the use of cells derived from a single source *in vitro* limit their biological relevance. Notably, neither study assessed cell viability or cytotoxicity under co-culture conditions, highlighting a key limitation that our model addresses by integrating four primary cell types from different donors with validated viability and cytotoxicity.

Mondadori et al. developed a microfluidic chip to model the synovium-cartilage interface, incorporating synovial and chondral compartments, an endothelial monolayer channel, and a dedicated synovial fluid channel. The system was populated with osteoarthritic synovial fibroblasts (SFbs) and articular chondrocytes (ACs) embedded in fibrin gel, while a perfusable endothelialized channel was established using human umbilical vein endothelial cells (HUVECs). This endothelial layer was designed to model vascularization and facilitate monocyte extravasation, simulating immune cell infiltration into the joint, a key feature in osteoarthritis pathology. To validate this, monocyte extravasation was assessed by perfusing TNF- $\alpha$  and chemokine gradients across the chip, which promoted migration through the endothelial layer into the synovial compartment. Further, OA synovial fluid from patient donors was used to trigger monocyte recruitment, highlighting the model's relevance in studying immune responses under inflammatory conditions (Mondadori et al., 2021). While this system provides a sophisticated platform for investigating immune-cell recruitment and synovial-chondral interactions, it focuses on cells from synovial and chondral tissues only, without inclusion of bone-derived cells or macrophages. Additionally, no direct validation of long-term cell viability or cytotoxicity was provided under co-culture conditions, limiting its applicability for comprehensive joint modeling.

Rothbauer et al. developed a joint-on-a-chip model to explore the reciprocal tissue crosstalk between synovial and chondral organoids. Their system featured two spatially separated hydrogel-based 3D organoid constructs, with synovial organoids composed of fibroblast-like synoviocytes (FLS) derived from rheumatoid arthritis (RA) patients undergoing synovectomy and chondral organoids formed using commercially available human primary chondrocytes. The co-culture was facilitated by soluble signaling between the two compartments, enabling tissue-level communication to study joint pathophysiology (Rothbauer et al., 2021). This model also demonstrates a sophisticated approach to modeling joint interactions; however, it is limited by a focus on synovial and chondral tissues exclusively, lacking the inclusion of bone-derived cells or macrophages. It is further limited by a reliance on a mixture of healthy and diseased cells within a single co-culture system, lacking clear “healthy” or “diseased” reference states between which to make comparisons of cell behavior. Additionally, no data were reported on cell viability, cytotoxicity, or functional stability of the co-culture system. These limitations highlight the distinct advantage of the model presented in this study, which incorporates four key joint cell types from different tissue sources, with validated viability and lack of cytotoxicity, and offers a more comprehensive platform for studying joint diseases.

Kubosch et al. investigated the paracrine interactions between human synovial mesenchymal stem cells (SMSCs) and chondrocytes using an *in vitro* Transwell® monolayer co-culture system (Kubosch et al., 2016). This approach enabled the examination of cellular crosstalk while maintaining physical separation between the two cell types. The SMSCs were isolated from synovial tissue collected during knee arthroscopy and arthroscopy procedures (n = 4, male/female 2/2). The chondrocytes were obtained from femoral heads during hip arthroplasty procedures (n = 6, male/female 5/1). While this study highlighted important paracrine interactions, it also lacked assessment of key functional metrics such as cell viability, cytotoxicity, or metabolic activity.

The present study represents a novel approach to OA modeling by co-culturing four distinct primary joint cell types—osteoblasts, chondrocytes, fibroblasts, and macrophages—within a unified microfluidic system with both healthy and diseased states governed by the cells within the system. This setup advances beyond prior models that typically incorporate only two cell types or rely on phenotypes derived from stem cells, offering a more physiologically relevant platform for joint research. The results presented here demonstrate the ability of the system presented in this study to sustain viability, metabolic activity, and membrane integrity across all cell types, providing a stable and functional co-culture environment.

However, certain limitations should be noted. First, human dermal fibroblasts (HDFs) were used instead of synovial fibroblasts, which may not fully capture the functional role of synovial cells in an articular joint. Second, the co-culture period was limited to 24 h, offering only a short-term perspective on cellular interactions, whereas longer-term studies may yield additional insights. Third, due to the technical requirements of the pre-conditioning period, primary chondrocytes were expanded and passaged prior to co-culture, which can alter their native phenotype. The absence of other relevant cell types, such as mast cells or plasma cells, as well as extracellular matrix (ECM) components, are also limitations of this initial validation study. Moreover, mechanical stress conditions were not applied; however, adjusting flow rates to higher levels within our microfluidic system could provide mechanical stimuli analogous to physiological stress conditions, representing an exciting avenue for future investigation. Such mechanical stimulation could reveal additional insights into joint pathophysiology and further increase the physiological relevance of the model. These limitations represent fertile opportunities for future studies building on the work presented here. Despite these limitations, our model provides the foundation for a robust and versatile platform for OA research, supporting future studies on disease pathophysiology and therapeutic testing.

Future work will focus on expanding the capabilities of our microfluidic co-culture system. A key priority is the quantification of key biomarkers, such as matrix metalloproteinases (MMPs) and inflammatory cytokines, to characterize the healthy and diseased profiles of our co-culture design. This will enable a more precise characterization of the pathophysiological differences induced by co-culture conditions. Additional studies incorporating fibroblasts of synovial origin and phenotype-modulating biophysical cues to recapitulate native tissue architectures are expected to further extend the translational potential of this model in the future. Ultimately, we aim to test potential drug candidates targeting critical OA pathways, leveraging the system as a preclinical screening tool. These advancements will support the development of translationally viable OA therapies and further validate the system's capacity as a predictive model for joint disease pathophysiology and therapeutic evaluation.

Moreover, future directions will include exploring the integration of additional cell types, such as mesenchymal stem cells (MSCs), to examine their dual roles in anti-inflammatory responses and senescence-associated secretory functions. The inclusion of other relevant immune cells, including mast cells and plasma cells, as well as extracellular matrix (ECM) components or mimetics and mechanical stimuli through varied

microfluidic flow rates or substrate stiffnesses, will also be investigated to further enhance the physiological recapitulation and translational applicability of our system.

## Conclusion

In this study, we present a microfluidic co-culture system using ibidi  $\mu$ -Slide I Luer microfluidic chips in which four cell types (osteoblasts, chondrocytes, fibroblasts, and two phenotypes of macrophages, M0 and M1) were integrated to simulate the complex cellular interactions of the human joint. Quiescent M0 macrophages represented the healthy model, while pro-inflammatory M1 macrophages simulated an inflammatory disease condition. This model will enable studies of different joint cells and the interactions between them in the context of both healthy and inflammatory environments. It is expected to provide a platform for OA and other rheumatic disease research, along with evaluating the potential efficacy of novel therapeutic approaches to treat these diseases. We observed that the present system-maintained cell viability, metabolic activity, and membrane integrity under co-culture conditions, revealed by NucBlue™/NucGreen™, PrestoBlue™, and LDH assays, respectively. No significant deleterious effects from crosstalk among cell types were observed, with increased metabolic activity consistently evident under co-culture conditions. These data could indicate that the model can mimic both healthy and diseased states without cytotoxicity and, therefore, is useful in studies of osteoarthritis pathophysiology. Furthermore, the stability of the system in inflammatory conditions indicated its potential for drug testing and therapeutic assessment of mainly treatments targeting inflammation. The model can be further optimized, but this microfluidic co-culture system paves the way toward more realistic models of the joint. Further studies could refine the system for high-throughput drug screening or investigate the use of this system for studying other inflammatory diseases or even other organs.

## Data availability statement

The raw data supporting the conclusions of this article will be made available by the authors, without undue reservation.

## Ethics statement

Ethical approval was not required for the studies on humans in accordance with the local legislation and institutional requirements because only commercially available established cell lines were used.

## References

- Awad, H., Ajalik, R., Alenchery, R., Linares, I., Wright, T., Miller, B., et al. (2023). Human tendon-on-a-chip for modeling vascular inflammatory fibrosis. *Res. Sq.* 14 (4), e2403116. doi:10.21203/rs.3.rs-372255/v1
- Bailey, K. N., and Alliston, T. (2022). At the crux of joint crosstalk: TGF $\beta$  signaling in the synovial joint. *Curr. Rheumatol. Rep.* 24 (6), 184–197. doi:10.1007/s11926-022-01074-6
- Banh, L., Cheung, K. K., Chan, M. W. Y., Young, E. W. K., and Viswanathan, S. (2022). Advances in organ-on-a-chip systems for modelling joint tissue and osteoarthritic diseases. *Osteoarthr. Cartil.* 30 (8), 1050–1061. doi:10.1016/j.joca.2022.03.012
- Baxter, E. W., Graham, A. E., Re, N. A., Carr, I. M., Robinson, J. I., Mackie, S. L., et al. (2020). Standardized protocols for differentiation of THP-1 cells to macrophages with distinct M(IFN $\gamma$ +LPS), M(IL-4) and M(IL-10) phenotypes. *J. Immunol. Methods* 478, 112721. doi:10.1016/j.jim.2019.112721
- Boncler, M., Róžalski, M., Krajewska, U., Podśędek, A., and Watala, C. (2014). Comparison of PrestoBlue and MTT assays of cellular viability in the assessment of anti-proliferative effects of plant extracts on human endothelial cells. *J. Pharmacol. Toxicol. Methods* 69 (1), 9–16. doi:10.1016/j.vascn.2013.09.003

## Author contributions

HM: Conceptualization, Data curation, Formal Analysis, Investigation, Methodology, Software, Validation, Visualization, Writing – original draft, Writing – review and editing. SW: Conceptualization, Data curation, Formal Analysis, Funding acquisition, Investigation, Methodology, Project administration, Resources, Software, Supervision, Validation, Visualization, Writing – original draft, Writing – review and editing.

## Funding

The author(s) declare that financial support was received for the research and/or publication of this article. This material is based upon work supported by the National Science Foundation under grant no. 2517512 (2234590).

## Conflict of interest

SW is an inventor on a patent that pertains to the methods described in this publication for which he is entitled to receive royalties and/or equity. US Patent No. 12098354B2 was issued to the South Dakota Board of Regents. In addition, SW is a partner in a company, CellField Technologies, Inc., that has licensed related technology from the South Dakota Board of Regents.

The remaining author declares that the research was conducted in the absence of any commercial or financial relationships that could be construed as a potential conflict of interest.

## Generative AI statement

The author(s) declare that Generative AI was used in the creation of this manuscript. Generative AI was used for editing grammar.

## Publisher's note

All claims expressed in this article are solely those of the authors and do not necessarily represent those of their affiliated organizations, or those of the publisher, the editors and the reviewers. Any product that may be evaluated in this article, or claim that may be made by its manufacturer, is not guaranteed or endorsed by the publisher.

- Cao, N., Wang, D., Liu, B., Wang, Y., Han, W., Tian, J., et al. (2023). Silencing of STUB1 relieves osteoarthritis via inducing NRF2-mediated M2 macrophage polarization. *Mol. Immunol.* 164, 112–122. doi:10.1016/j.molimm.2023.11.010
- Cope, P. J., Ourradi, K., Li, Y., and Sharif, M. (2019). Models of osteoarthritis: the good, the bad and the promising. *Osteoarthr. Cartil.* 27 (2), 230–239. doi:10.1016/j.joca.2018.09.016
- Cutolo, M., Campitiello, R., Gotelli, E., and Soldano, S. (2022). The role of M1/M2 macrophage polarization in rheumatoid arthritis synovitis. *Front. Immunol.* 13, 867260. doi:10.3389/fimmu.2022.867260
- Domínguez-Oliva, A., Hernández-Ávalos, I., Martínez-Burnes, J., Olmos-Hernández, A., Verduzco-Mendoza, A., and Mota-Rojas, D. (2023). The importance of animal models in biomedical research: current insights and applications. *Animals* 13 (7), 1223. doi:10.3390/ani13071223
- Dou, H., Wang, S., Hu, J., Song, J., Zhang, C., Wang, J., et al. (2023). Osteoarthritis models: from animals to tissue engineering. *J. Tissue Eng.* 14, 20417314231172584. doi:10.1177/20417314231172584
- Finsson, K. W., Chi, Y., Bou-Gharios, G., Leask, A., and Philip, A. (2012). TGF- $\beta$  signaling in cartilage homeostasis and osteoarthritis. *Front. Biosci. Sch.* 4 (1), 251–268. doi:10.2741/s266
- Galli, S. J., Gaudenzio, N., and Tsai, M. (2020). Mast cells in inflammation and disease: recent progress and ongoing concerns. *Annu. Rev. Immunol.* 38, 49–77. doi:10.1146/annurev-immunol-071719-094903
- Goers, L., Freemont, P., and Polizzi, K. M. (2014). Co-culture systems and technologies: taking synthetic biology to the next level. *J. R. Soc. Interface* 11 (96), 20140065. doi:10.1098/rsif.2014.0065
- Grässel, S., and Muschter, D. (2020). Recent advances in the treatment of osteoarthritis. *F1000Res* 9, 325. doi:10.12688/f1000research.22115.1
- Guo, J., Huang, X., Dou, L., Yan, M., Shen, T., Tang, W., et al. (2022). Aging and aging-related diseases: from molecular mechanisms to interventions and treatments. *Signal Transduct. Target. Ther.* 7 (1), 391. doi:10.1038/s41392-022-01251-0
- Haltmayer, E., Ribitsch, I., Gabner, S., Rosser, J., Gueltekin, S., Peham, J., et al. (2019). Co-culture of osteochondral explants and synovial membrane as *in vitro* model for osteoarthritis. *PLoS One* 14 (4), e0214709. doi:10.1371/journal.pone.0214709
- Hao, G., Han, S., Xiao, Z., Shen, J., Zhao, Y., and Hao, Q. (2024). Synovial mast cells and osteoarthritis: current understandings and future perspectives. *Heliyon*, 10(24), e41003. doi:10.1016/j.heliyon.2024.e41003
- He, Y., Li, Z., Alexander, P. G., Ocasio-Nieves, B. D., Yocum, L., Lin, H., et al. (2020). Pathogenesis of osteoarthritis: risk factors, regulatory pathways in chondrocytes, and experimental models. *Biol. (Basel)* 9 (8), 194. doi:10.3390/biology9080194
- Hofer, M., and Lutolf, M. P. (2021). Engineering organoids. *Nat. Rev. Mater* 6 (5), 402–420. doi:10.1038/s41578-021-00279-y
- Irani, A. A., Schechter, N. M., Craig, S. S., DeBlois, G., and Schwartz, L. B. (1986). Two types of human mast cells that have distinct neutral protease compositions. *Proc. Natl. Acad. Sci.* 83 (12), 4464–4468. doi:10.1073/pnas.83.12.4464
- Kao, C.-Y., Mills, J. A., Burke, C. J., Morse, B., and Marques, B. F. (2023). Role of cytokines and growth factors in the manufacturing of iPSC-derived allogeneic cell therapy products. *Biology* 12 (5), 677. doi:10.3390/biology12050677
- Kilinc, E., Torun, I. E., Cetinkaya, A., and Tore, F. (2022). Mast cell activation ameliorates pentylenetetrazole-induced seizures in rats: the potential role for serotonin. *Eur. J. Neurosci.* 55(9–10), 2912–2924. doi:10.1111/ejn.15145
- Klabukov, I., Atiakshin, D., Kogan, E., Ignatyuk, M., Krashenninnikov, M., Zharkov, N., et al. (2023). Post-implantation inflammatory responses to xenogeneic tissue-engineered cartilage implanted in rabbit trachea: the role of cultured chondrocytes in the modification of inflammation. *Int. J. Mol. Sci.* 24 (23), 16783. doi:10.3390/ijms242316783
- Kubosch, E. J., Heidt, E., Bernstein, A., Böttiger, K., and Schmal, H. (2016). The transwell coculture of human synovial mesenchymal stem cells with chondrocytes leads to self-organization, chondrogenic differentiation, and secretion of TGF $\beta$ . *Stem Cell Res. and Ther.* 7 (1), 64. doi:10.1186/s13287-016-0322-3
- Li, Z. A., Sant, S., Cho, S. K., Goodman, S. B., Bunnell, B. A., Tuan, R. S., et al. (2023). Synovial joint-on-a-chip for modeling arthritis: progress, pitfalls, and potential. *Trends Biotechnol.* 41 (4), 511–527. doi:10.1016/j.tibtech.2022.07.011
- Lin, H., Lozito, T. P., Alexander, P. G., Gottardi, R., and Tuan, R. S. (2014). Stem cell-based microphysiological osteochondral system to model tissue response to interleukin-1 $\beta$ . *Mol. Pharm.* 11 (7), 2203–2212. doi:10.1021/mp500136b
- Lin, Z., Li, Z., Li, E. N., Li, X., Del Duke, C. J., Shen, H., et al. (2019). Osteochondral tissue chip derived from iPSCs: modeling OA pathologies and testing drugs. *Front. Bioeng. Biotechnol.* 7, 411. doi:10.3389/fbioe.2019.00411
- Loeser, R. F., Goldring, S. R., Scanzello, C. R., and Goldring, M. B. (2012). Osteoarthritis: a disease of the joint as an organ. *Arthritis Rheum.* 64 (6), 1697–1707. doi:10.1002/art.34453
- Long, H., Liu, Q., Yin, H., Wang, K., Diao, N., Zhang, Y., et al. (2022). Prevalence trends of site-specific osteoarthritis from 1990 to 2019: findings from the global burden of disease study 2019. *Arthritis Rheumatol.* 74 (7), 1172–1183. doi:10.1002/art.42089
- Makarczyk, M. J., Li, Z. A., Yu, I., Yagi, H., Zhang, X., Yocum, L., et al. (2023). Creation of a knee joint-on-a-chip for modeling joint diseases and testing drugs. *J. Vis. Exp.* 191, 64186. doi:10.3791/64186
- Malfait, A. M., and Little, C. B. (2015). On the predictive utility of animal models of osteoarthritis. *Arthritis Res. Ther.* 17 (1), 225. doi:10.1186/s13075-015-0747-6
- Martin, J. A., and Buckwalter, J. A. (2002). Aging, articular cartilage chondrocyte senescence and osteoarthritis. *Biogerontology* 3 (5), 257–264. doi:10.1023/a:1020185404126
- Martin-Navarro, C. M., López-Arencibia, A., Sifaoui, I., Reyes-Batlle, M., Cabello-Vilchez, A. M., Maciver, S., et al. (2014). PrestoBlue<sup>®</sup> and AlamarBlue<sup>®</sup> are equally useful as agents to determine the viability of *Acanthamoeba trophozoites*. *Exp. Parasitol.* 145 (Suppl. 1), S69–S72. doi:10.1016/j.exppara.2014.03.024
- McNerney, M. P., Doiron, K. E., Ng, T. L., Chang, T. Z., and Silver, P. A. (2021). Theranostic cells: emerging clinical applications of synthetic biology. *Nat. Rev. Genet.* 22 (11), 730–746. doi:10.1038/s41576-021-00383-3
- Mondadori, C., Palombella, S., Salehi, S., Talò, G., Visone, R., Rasponi, M., et al. (2021). Recapitulating monocyte extravasation to the synovium in an organotypic microfluidic model of the articular joint. *Biofabrication* 13 (4), 045001. doi:10.1088/1758-5090/ac0c5e
- Palasantzas, V. E. J. M., Tamargo-Rubio, I., Le, K., Slager, J., Wijmenga, C., Jonkers, I. H., et al. (2023). iPSC-derived organ-on-a-chip models for personalized human genetics and pharmacogenomics studies. *Trends Genet.* 39 (4), 268–284. doi:10.1016/j.tig.2023.01.002
- Perisin, M. A., and Sund, C. J. (2018). Human gut microbe co-cultures have greater potential than monocultures for food waste remediation to commodity chemicals. *Sci. Rep.* 8 (1), 15594. doi:10.1038/s41598-018-33733-z
- Pirosa, A., Tankus, E. B., Mainardi, A., Occhetta, P., Dönges, L., Baum, C., et al. (2021). Modeling *in vitro* osteoarthritis phenotypes in a vascularized bone model based on a bone-marrow derived mesenchymal cell line and endothelial cells. *Int. J. Mol. Sci.* 22 (17), 9581. doi:10.3390/ijms22179581
- Rothbauer, M., Byrne, R. A., Schobesberger, S., Olmos Calvo, I., Fischer, A., Reihs, E. I., et al. (2021). Establishment of a human three-dimensional chip-based chondro-synovial coculture joint model for reciprocal cross talk studies in arthritis research. *Lab. Chip* 21 (21), 4128–4143. doi:10.1039/d1lc00130b
- Salgado, C., Jordan, O., and Allémann, E. (2021). Osteoarthritis *in vitro* models: applications and implications in development of intra-articular drug delivery systems. *Pharmaceutics* 13 (1), 60. doi:10.3390/pharmaceutics13010060
- Shen, J., Li, J., Wang, B., Jin, H., Wang, M., Zhang, Y., et al. (2013). Deletion of the transforming growth factor  $\beta$  receptor type II gene in articular chondrocytes leads to a progressive osteoarthritis-like phenotype in mice. *Arthritis and Rheumatism*, 65(12), 3107–3119. doi:10.1002/art.38122
- Swearengen, J. R. (2018). Choosing the right animal model for infectious disease research. *Anim. Model Exp. Med.* 1 (2), 100–108. doi:10.1002/ame2.12020
- Tong, L., Yu, H., Huang, X., Shen, J., Xiao, G., Chen, L., et al. (2022). Current understanding of osteoarthritis pathogenesis and relevant new approaches. *Bone Res.* 10 (1), 60. doi:10.1038/s41413-022-00226-9
- Wang, N., Liang, H., and Zen, K. (2014). Molecular mechanisms that influence the macrophage m1-m2 polarization balance. *Front. Immunol.* 5, 614. doi:10.3389/fimmu.2014.00614
- Weiskirchen, S., Schröder, S. K., Buhl, E. M., and Weiskirchen, R. (2023). A beginner's guide to cell culture: practical advice for preventing needless problems. *Cells* 12 (5), 682. doi:10.3390/cells12050682
- Xie, X., Zhu, J., Hu, X., Dai, L., Fu, X., Zhang, J., et al. (2018). A co-culture system of rat synovial stem cells and meniscus cells promotes cell proliferation and differentiation as compared to mono-culture. *Sci. Rep.* 8 (1), 7693. doi:10.1038/s41598-018-25709-w
- Xu, M., McCanna, D. J., and Sivak, J. G. (2015). Use of the viability reagent PrestoBlue in comparison with alamarBlue and MTT to assess the viability of human corneal epithelial cells. *J. Pharmacol. Toxicol. Methods* 71, 1–7. doi:10.1016/j.vascn.2014.11.003
- Zaki, S., Blaker, C. L., and Little, C. B. (2022). OA foundations – experimental models of osteoarthritis. *Osteoarthr. Cartil.* 30(3), 357–380. doi:10.1016/j.joca.2021.03.024
- Zhang, H.-W., Xie, G.-H., Ren, X.-H., Yang, Y.-Z., Song, Q., and Yu, H. (2020). Bursicon homodimers induce the innate immunity via Relish in *Procambarus clarkii*. *Fish and Shellfish Immunol.* 99, 555–561. doi:10.1016/j.fsi.2020.02.053
- Zhen, G., and Cao, X. (2014). Targeting TGF $\beta$  signaling in subchondral bone and articular cartilage homeostasis. *Trends Pharmacol. Sci.* 35(5), 227–236. doi:10.1016/j.tips.2014.03.005
- Zhou, T., Yuan, Z., Weng, J., Pei, D., Du, X., He, C., et al. (2021). Challenges and advances in clinical applications of mesenchymal stromal cells. *J. Hematol. and Oncol.* 14 (1), 24. doi:10.1186/s13045-021-01037-x